Please cite this article in press as: Squadrito et al., Endogenous RNAs Modulate MicroRNA Sorting to Exosomes and Transfer to Acceptor Cells, Cell Reports (2014), http://dx.doi.org/10.1016/j.celrep.2014.07.035

Cell Reports
Article

Endogenous RNAs Modulate MicroRNA Sorting to Exosomes and Transfer to Acceptor Cells

Mario Leonardo Squadrito,[1,4] Caroline Baer,[1,4] Frédéric Burdet,[2] Claudio Maderna,[1] Gregor D. Gilfillan,[3] Robert Lyle,[3] Mark Ibberson,[2] and Michele De Palma[1,*]
[1]Swiss Institute for Experimental Cancer Research (ISREC), School of Life Sciences, École Polytechnique Fédérale de Lausanne (EPFL), 1015 Lausanne, Switzerland
[2]Vital-IT, Swiss Institute of Bioinformatics (SIB), 1015 Lausanne, Switzerland
[3]Department of Medical Genetics and Norwegian High-Throughput Sequencing Centre (NSC), Oslo University Hospital, Kirkeveien 166, 0407 Oslo, Norway
[4]Co-first author
*Correspondence: michele.depalma@epfl.ch
http://dx.doi.org/10.1016/j.celrep.2014.07.035

SUMMARY

MicroRNA (miRNA) transfer via exosomes may mediate cell-to-cell communication. Interestingly, specific miRNAs are enriched in exosomes in a cell-type-dependent fashion. However, the mechanisms whereby miRNAs are sorted to exosomes and the significance of miRNA transfer to acceptor cells are unclear. We used macrophages and endothelial cells (ECs) as a model of heterotypic cell communication in order to investigate both processes. RNA profiling of macrophages and their exosomes shows that miRNA sorting to exosomes is modulated by cell-activation-dependent changes of miRNA target levels in the producer cells. Genetically perturbing the expression of individual miRNAs or their targeted transcripts promotes bidirectional miRNA relocation from the cell cytoplasm/P bodies (sites of miRNA activity) to multivesicular bodies (sites of exosome biogenesis) and controls miRNA sorting to exosomes. Furthermore, the use of *Dicer*-deficient cells and reporter lentiviral vectors (LVs) for miRNA activity shows that exosomal miRNAs are transferred from macrophages to ECs to detectably repress targeted sequences.

INTRODUCTION

MicroRNAs (miRNAs/miRs) are a class of small noncoding RNAs that regulate gene expression at the posttranscriptional level (Yates et al., 2013). Precursor miRNAs are exported from the cell nucleus to the cytoplasm, where they are processed into mature miRNAs by the enzyme DICER. Upon loading into the RNA-induced silencing complex (RISC), miRNAs bind the 3′ UTR of target transcripts to fine-tune their expression via degradation and/or translational repression (Bartel, 2009). Several hundreds of mature miRNAs have been identified in metazoans, many of which are predicted to modulate the expression of multiple gene transcripts (Lewis et al., 2005). miRNAs are also detected in extracellular compartments, such as body fluids, either in complex with proteins of the argonaute (AGO) family or loaded into exosomes (Turchinovich et al., 2012). Exosomes are microvesicles produced by multiple cell types, which originate from the fusion of late endosomes/multivesicular bodies (MVBs) with the cell plasma membrane. Upon their release in the extracellular environment, exosomes can fuse with live cells, either paracrinally or endocrinally, and transfer their cargo of proteins, lipids, and RNAs to the acceptor cells (Simons and Raposo, 2009).

RNA sequencing (RNA-seq) has shown that miRNAs are abundant in exosomes. Notably, the miRNA repertoire of exosomes may differ from that of the producer cell (Gibbings et al., 2009; Guduric-Fuchs et al., 2012; Nolte-'t Hoen et al., 2012; Simons and Raposo, 2009; Skog et al., 2008; Valadi et al., 2007). This finding suggests that the sorting of specific miRNA species to exosomes may be actively regulated, although the underlying mechanisms remain largely unknown. Both the process of MVB/exosome biogenesis and miRNA-sequence-specific determinants may modulate miRNA sorting to exosomes. Members of the endosomal sorting complex required for transport (ESCRT) play crucial functions in MVB biogenesis and exocytosis. However, knockdown of ESCRT proteins does not affect miRNA sorting to exosomes (Kosaka et al., 2010). A recent study identified a specific 4 nt sequence (GGAG) that is overrepresented in miRNAs that are enriched in T cell-derived exosomes. The GGAG motif is bound by sumoylated hnRNPA2B1 (a heterogeneous nuclear riboprotein), which directs miRNA trafficking to MVBs and their secretion via exosomes (Villarroya-Beltri et al., 2013). Thus, specific motifs present in certain miRNAs may guide their sorting to exosomes through the interaction with specific chaperon proteins.

Multiple cell types, such as immune cells, endothelial cells (ECs), and cancer cells, can internalize exosomes secreted by other cells. Several studies have proposed that the transfer of exosomal miRNAs may modulate the biological functions of the acceptor cells (Hergenreider et al., 2012; Mittelbrunn et al., 2011; Montecalvo et al., 2012; Ramachandran and Palanisamy,

Please cite this article in press as: Squadrito et al., Endogenous RNAs Modulate MicroRNA Sorting to Exosomes and Transfer to Acceptor Cells, Cell Reports (2014), http://dx.doi.org/10.1016/j.celrep.2014.07.035

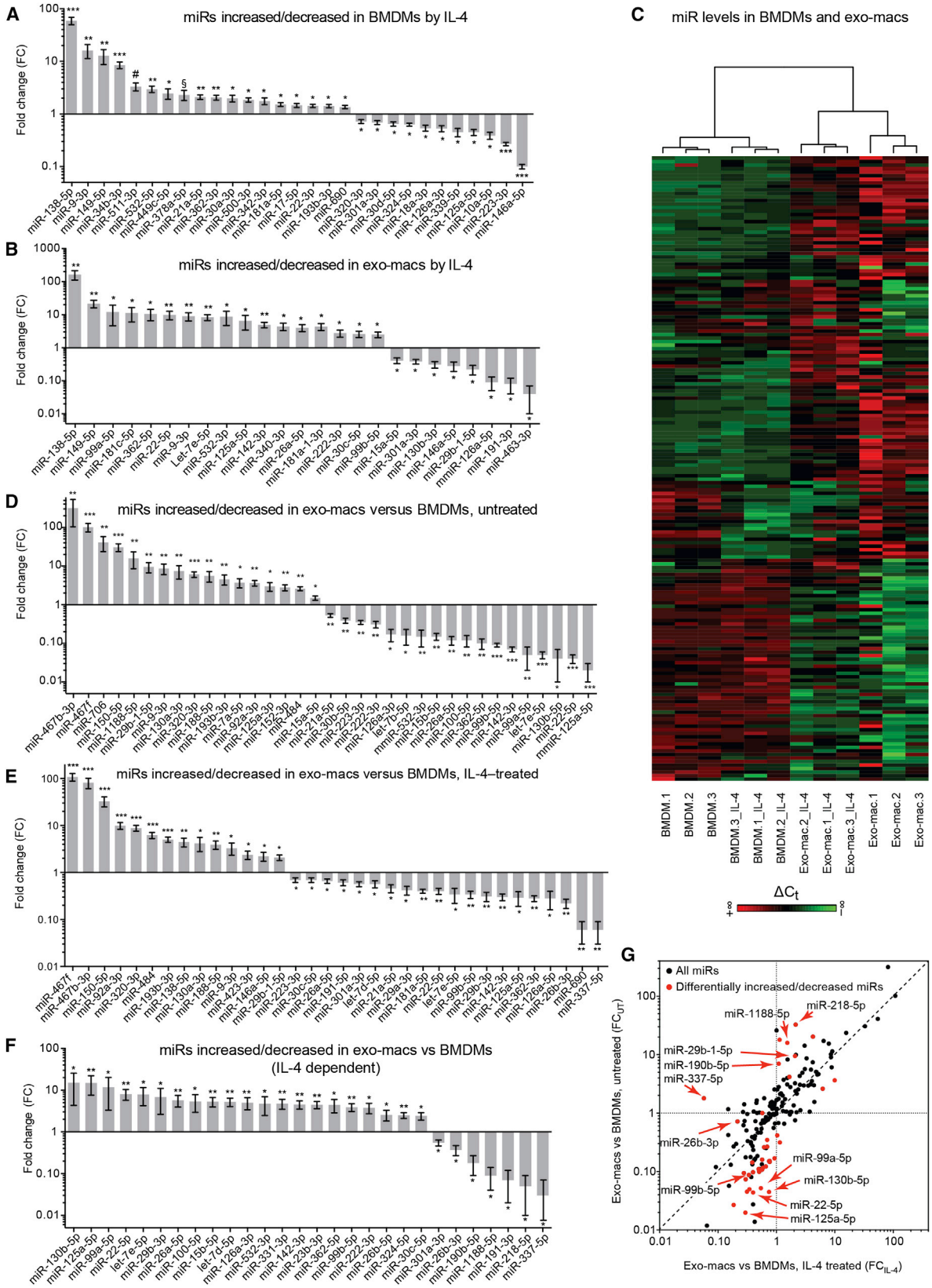

(legend on next page)

2012; Valadi et al., 2007). Nevertheless, distinguishing exogenous miRNA transfer/activity from the endogenous activation of miRNA transcription/activity consequent to exosome-cell physical interactions may prove challenging; therefore, definitive evidence for the robustness of transfer of miRNA activity from exosomes to acceptor cells remains scant. In this study, we employed macrophages and ECs as a model system to investigate the molecular determinants of miRNA sorting to exosomes and transfer to acceptor cells. Our findings indicate that miRNA sorting to exosomes is regulated, at least in part, by cell-activation-dependent changes of targeted transcript levels in the cell cytoplasm. Furthermore, by employing sensitive reporter lentiviral vectors (LVs), we show that transfer of miRNA activity from macrophage-derived exosomes has the potential to detectably modulate the gene expression and biology of acceptor ECs.

RESULTS

Cell-Activation-Dependent miRNA Enrichment in Exosomes

We isolated microvesicles secreted by colony-stimulating factor 1 (CSF-1)-induced bone marrow-derived macrophages (BMDMs) that were either untreated (UT) or stimulated with interleukin-4 (IL-4). As expected, IL-4 increased the expression of the "alternative macrophage activation" genes *Arg1*, *CD163*, and *Mrc1* in BMDMs (Figure S1A). BMDM-derived microvesicles were highly enriched in particles that had features of exosomes, as shown by physical size analysis by dynamic light scattering (Figure S1B) and protein content by western blotting analysis (Figure S1C). From here on, we refer to macrophage-derived exosomes as "exo-macs."

We profiled the miRNA transcriptome of BMDMs and their exo-macs, either UT (n = 3) or IL-4 treated (IL-4; n = 3), by low-density quantitative PCR (qPCR) arrays. A total of 178 (29%) of the 618 miRNAs present in the arrays were detected in at least two out of three biological replicates of both BMDMs and exo-macs (Table S1). After quantile normalization of the data, 31 miRNAs (5%) were differentially expressed in IL-4-treated versus UT BMDMs (Figure 1A; Table S2A), including miR-138-5p, miR-9-3p (both upregulated; fold-change [FC] = 59 and 16, respectively), miR-146a-5p, and miR-223-3p (both downregulated; FC = 0.10 and 0.27, respectively). We also identified 40 miRNAs (6%) that were relatively increased or decreased in the exo-macs by IL-4 (Figure 1B; Table S2B). These data indicate that IL-4 modulates the expression and/or enrichment of a subset of miRNAs in BMDMs and their exo-macs.

The global miRNA profile greatly differed in BMDMs and exo-macs, regardless of IL-4 stimulation, as shown by the unsupervised hierarchical clustering of the data (Figure 1C). Of the 178 miRNAs detected in all samples, 90 (51%) and 101 (57%) were relatively increased/decreased in the exo-macs compared to UT and IL-4-treated BMDMs, respectively (Figures 1D and 1E; Tables S2C and S2D). Among the miRNAs enriched in the exo-macs were miR-150-5p, miR-146a-5p, miR-320-3p, miR-467b-3p, and miR-467f; of these, miR-150-5p, miR-146a-5p, and miR-320-3p were previously found to be enriched in exosomes derived from distinct cell types (Guduric-Fuchs et al., 2012). Furthermore, 39 miRNAs were relatively increased or decreased in the exo-macs versus BMDMs in an IL-4-dependent manner (e.g., more enriched in exo-macs by IL-4; Figures 1F and 1G; Table S2E).

Although our experimental conditions and analyses cannot measure absolute miRNA abundance in exo-macs and producer BMDMs, they indicate that (1) selected miRNAs are differentially represented in exo-macs and BMDMs (relative to the global miRNA repertoire), and (2) miRNA enrichment in exo-macs is not only miRNA-specific but also dependent on the cell activation state. From here on, we refer to miRNAs contained in exo-macs as "exo-miRNAs."

Artificially Perturbing miRNA or Targeted Transcript Levels Modulates miRNA Sorting to MVBs and Exosomes

Little is known of the molecular regulation of miRNA sorting to exosomes. In order to explore potential mechanisms, we first generated miRNA-deficient BMDMs by transducing bone marrow-derived cells from *Dicer*$^{fl/fl}$ mice with a Cre-expressing LV (Figure S2A). We then analyzed a panel of miRNAs in either *Dicer*$^{fl/fl}$ or *Dicer*$^{-/-}$ BMDMs, and their secreted exo-macs, at day 12 posttransduction, a time point when *Dicer* had been efficiently (albeit nonexhaustively) deleted in the LV-transduced BMDMs (Figure S2B). Intriguingly, miRNA depletion was substantially more prominent in the exo-macs than in the producer, *Dicer*$^{-/-}$ cells, regardless of IL-4 stimulation (Figures 2A and 2B). This was true for each miRNA analyzed and was independent of the expression level of the miRNA in *Dicer*-proficient BMDMs. Thus, upon acute *Dicer* deletion in BMDMs, a moderate miRNA decrease in the cells is associated with a more prominent miRNA depletion in the exo-macs.

To further investigate this phenomenon, we asked whether changes in the abundance of a given miRNA and/or its targets (including artificial and natural targets) could alter miRNA sorting to the exosomes. In order to standardize experimental conditions, we generated a macrophage cell line by immortalizing

Figure 1. miRNA Analysis in BMDMs and Their Exo-Macs

(A and B) Selected miRNAs (indicated as miRs) increased or decreased in BMDMs (A) and exo-macs (B) by IL-4, analyzed by low-density TaqMan arrays. Data show fold-change (FC) in IL-4-treated versus UT BMDMs/exo-macs (FC = $2^{-\Delta Ct}$, with C_t values normalized by quantile method; mean ± SEM, n = 3). Statistical analysis by moderated t-statistics adjusted for false discovery rate (FDR); *p < 0.05; **p < 0.01; ***p < 0.001, §p = 0.0502. # indicates a miRNA not present in the array and measured separately (FC = $2^{-\Delta\Delta Ct}$, with C_t values normalized to U6; mean ± SEM, n = 3; p = 0.0134; statistical analysis by unpaired Student's t test).

(C) Mean-centered heatmap showing unsupervised hierarchical clustering of miRNA levels in UT (BMDM.1-3) and IL-4-treated (BMDM.1-3_IL-4) BMDMs and their exo-macs (exo-mac.1-3 and exo-mac.1-3_IL-4).

(D and E) Selected miRNAs increased or decreased in exo-macs versus BMDMs, either UT (D) or IL-4 treated (E). Analysis as in (A) and (B).

(F and G) Differential miRNA increase/decrease in exo-macs versus BMDMs by IL-4. (F) Selected miRNAs increased or decreased in exo-macs versus BMDMs by IL-4. Data are shown as FC between FC_{IL-4} and FC_{UT} (mean ± SEM, n = 3). Statistical analysis as in (A) and (B). (G) FC of miRNA levels in exo-macs versus UT (FC_{UT}, y axis) or IL-4-treated (FC_{IL-4}, x axis) BMDMs. miRNAs significantly increased/decreased are shown in red (adjusted p < 0.05; statistical analysis as in A and B).

Please cite this article in press as: Squadrito et al., Endogenous RNAs Modulate MicroRNA Sorting to Exosomes and Transfer to Acceptor Cells, Cell Reports (2014), http://dx.doi.org/10.1016/j.celrep.2014.07.035

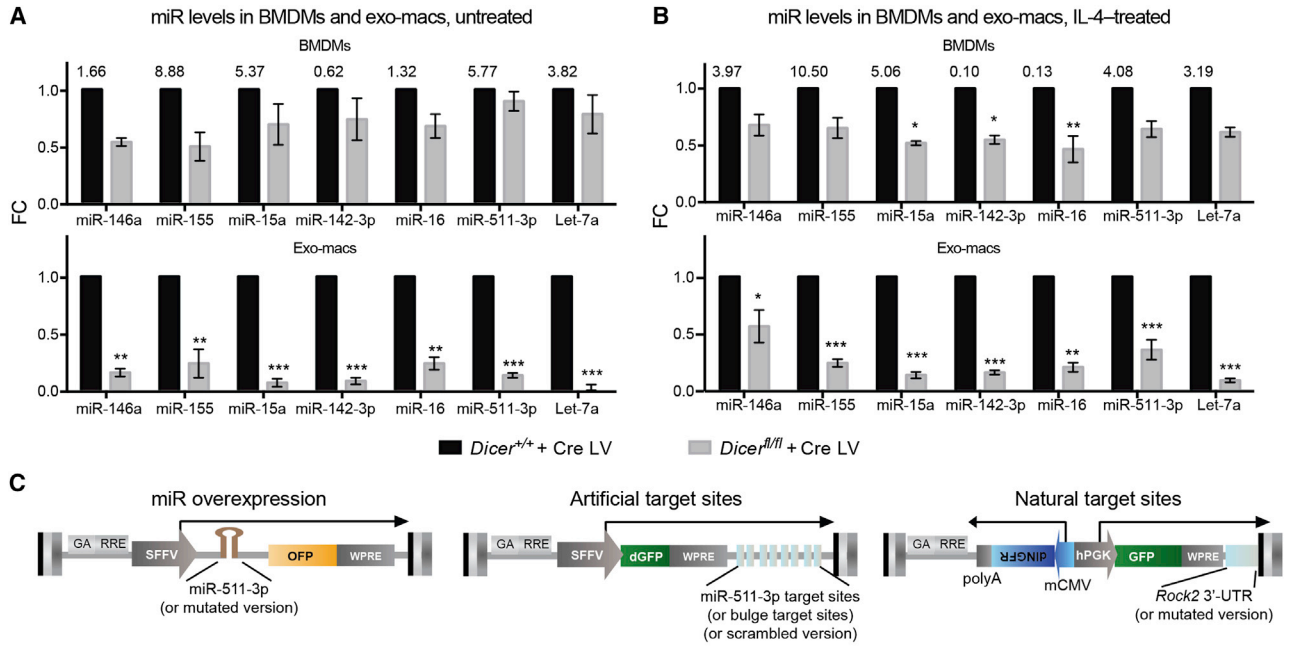

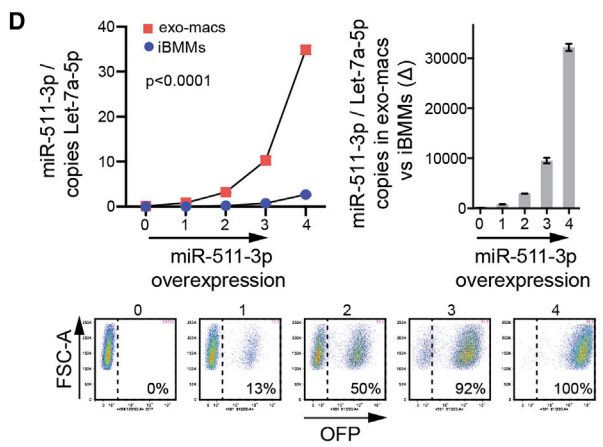

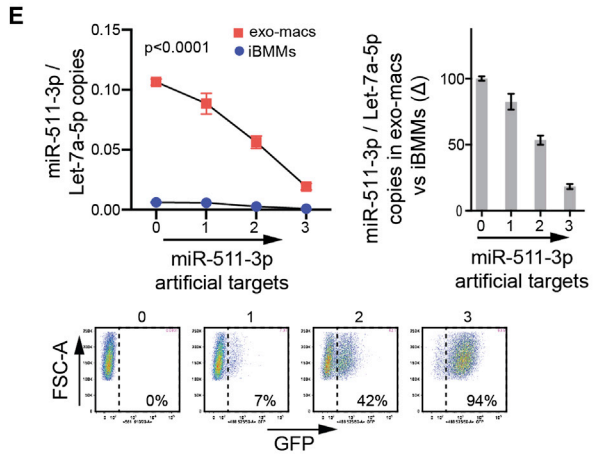

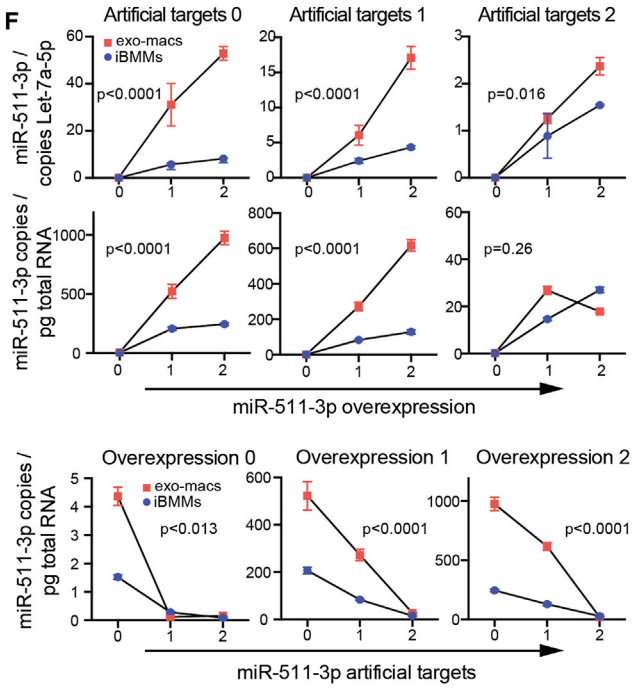

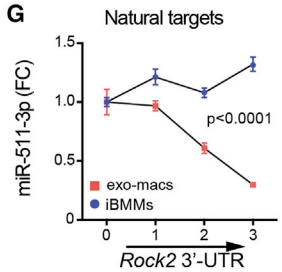

(legend on next page)

Dicer$^{fl/fl}$ BMDMs with an LV expressing the SV40 large T antigen (Figure S2A). A clonal population of immortalized BMDMs (iBMMs) expressed all analyzed macrophage-specific markers, could be polarized in response to cytokine (IL-4 or LPS plus IFN-γ) stimulation, and was dependent on CSF-1 for survival and growth (Figures S2C–S2F). Furthermore, iBMMs produced bona fide exo-macs, as shown by physical size analysis by dynamic light scattering (Figure S2G), morphology by transmission electron microscopy (Figure S2H), and protein content by western blotting analysis (Figure S2I). Thus, iBMMs represent a suitable surrogate cell line for primary BMDMs.

UT iBMMs express low levels of miR-511-3p, a macrophage-specific miRNA that is induced by IL-4 (Squadrito et al., 2012). We then transduced iBMMs with increasing doses of an LV overexpressing miR-511-3p (Squadrito et al., 2012 and Figure 2C) and analyzed miR-511-3p levels in iBMMs and their exo-macs. Upon increasing overexpression, miR-511-3p levels surged to a greater extent in the exo-macs than in the iBMMs (Figure 2D). Thus, partial miRNA depletion strongly limits (see Figures 2A and 2B) while miRNA overexpression strongly enhances miRNA sorting to exosomes. In a series of parallel experiments, we analyzed the effects of artificially increasing the cellular levels of miR-511-3p target sequences. To this aim, we transduced the iBMMs with increasing doses of an LV expressing eight copies of artificial sequences with perfect complementarity to miR-511-3p (Figure 2C). Robust overexpression of artificial miRNA target sequences detectably decreased endogenous miR-511-3p levels in the iBMMs (Figure 2E), likely through a "miRNA sponge effect" (Brown and Naldini, 2009; Denzler et al., 2014; Gentner et al., 2009; Mullokandov et al., 2012). However, miR-511-3p levels decreased in the exo-macs to a greater extent than in the iBMMs. Finally, iBMMs engineered to overexpress increasing levels of both miR-511-3p and its target sequences by sequential LV transduction showed that miRNA transfer to exo-macs is controlled by the relative levels of the miRNA and its target sequences in the cell (Figure 2F). Indeed, quantification of miR-511-3p, either after normalization to Let-7a-5p or by absolute copy-number analysis, indicated that maximal overexpression of miR-511-3p target sequences ("artificial targets 2" in Figure 2F) reversed the exosomal enrichment of miR-511-3p that was induced by its overexpression.

While artificial (perfectly complementary) sequences may promote miRNA-dependent cleavage of the target, natural (partially complementary) sequences may cause mRNA destabilization and translation inhibition (Ameres et al., 2007). We then employed natural target sequences for miR-511-3p. We previously validated *Rock2* as a natural target of miR-511-3p (Squadrito et al., 2012). We then transduced iBMMs with increasing doses of an LV expressing a fragment of the *Rock2* 3′ UTR that encompasses target sites for miR-511-3p (*Rock2* 3′UTR LV; Figure 2C). As a control LV, we used *Rock2* 3′ UTR sequences with mutated miR-511-3p binding sites (Squadrito et al., 2012). Whereas natural target sequences did not "sponge" endogenous miR-511-3p detectably in the cells (contrary to artificial sequences; see Figures 2D–2F), they efficiently decreased miR-511-3p levels in the exo-macs (Figure 2G). Taken together, these findings indicate that artificially increasing the abundance of miRNA target sequences limits miRNA levels in the exosomes more markedly than in the producer cells.

MVBs are complex organelles that function as sites of exosome biogenesis (Simons and Raposo, 2009). Based on our finding that artificially increasing the expression of a given miRNA disproportionally increases its levels in the exosomes, we hypothesized that artificially overexpressed miRNAs would also enrich in MVBs. We then performed subcellular fractionation of iBMMs (Gibbings et al., 2009; Stalder et al., 2013) and obtained nine distinct subcellular fractions that were analyzed by western blotting (Figures 3A and S3A). MVBs were enriched in fraction 3 and, to a lesser extent, fractions 2 and 4, as shown by expression of the tetraspanin CD81 (Figure 3A). Fractions 4 to 9 were enriched in endoplasmic reticulum (ER), as shown by expression of calnexin (CNX), whereas fraction 1 and, to a lesser extent, fraction 2 were enriched in P bodies markers, such as AGO2, GW182, and DCP1A, indicative of sites of miRNA activity (Liu et al., 2005). We then transduced iBMMs with a high dose of an LV overexpressing miR-511-3p, or a mutated form (miR-511-3p-mut; Figure S3B; Squadrito et al., 2012), and performed subcellular fractionation. In iBMMs expressing miR-511-3p-mut, endogenous miR-511-3p was detectable, albeit at varying levels, in each fraction (Figure 3B). Overexpressing miR-511-3p increased its levels in all subcellular fractions (data not shown); however, it did so more prominently in the MVB-enriched fraction 3 compared to the other fractions. Conversely, overexpressing artificial (perfectly complementary) or bulge (partially complementary) target sequences for miR-511-3p in the iBMMs (Figure S3B) significantly increased miR-511-3p levels in the P bodies-enriched fraction 1 (Figures 3C and 3D).

Together, these data indicate that artificially increasing the cellular levels of a miRNA or its target sequences favors miRNA

Figure 2. Changes of miRNA Levels or Their Target Sequences Control miRNA Sorting to Exo-Macs

(A and B) TaqMan analysis of selected miRNAs (indicated as miRs) in *Dicer*$^{+/+}$ and *Dicer*$^{fl/fl}$ BMDMs transduced with a Cre-expressing LV, and their exo-macs, either UT (A) or IL-4 treated (B). Data show FC (FC = $2^{-\Delta\Delta Ct}$, with C_t values normalized to U6; mean ± SEM, n = 2–3) versus LV-transduced *Dicer*$^{+/+}$ BMDMs (black bars, upper panels) or their exo-macs (black bars, bottom panels). In the top panels, miRNA ΔC_t values (versus U6) are indicated for BMDMs. Statistical analysis by two-way ANOVA, with Sidak's multiple comparisons test.

(C) Schematics of proviral LVs.

(D and E) Top graphs show miR-511-3p levels (D, normalized to Let-7a-5p; E, difference between normalized levels in exo-macs versus cells) in iBMMs and exo-macs. iBMMs were transduced with increasing doses (D, 1–4; E, 1–3) of LVs either overexpressing miR-511-3p (D) or its artificial target sequences (E); dose 0 indicates untransduced iBMMs. FACS dot plots on the bottom show iBMMs transduced as indicated. Statistical analysis by analysis of covariance (ANCOVA).

(F) miR-511-3p levels in iBMMs and exo-macs. iBMMs were cotransduced with increasing doses of LVs overexpressing miR-511-3p or its artificial target sequences, as indicated. miR-511-3p levels were either normalized to Let-7a-5p or shown as absolute miRNA copies per pg of total RNA. Statistical analysis by ANCOVA.

(G) miR-511-3p levels normalized to Let-7a-5p in iBMMs and exo-macs. iBMMs were transduced with increasing doses (1–3) of an LV expressing a fragment of the *Rock2* 3′ UTR. Data show FC versus exo-macs or iBMMs transduced with a mutated *Rock2* 3′ UTR (mean ± SEM, n = 3). Statistical analysis by ANCOVA.

Please cite this article in press as: Squadrito et al., Endogenous RNAs Modulate MicroRNA Sorting to Exosomes and Transfer to Acceptor Cells, Cell Reports (2014), http://dx.doi.org/10.1016/j.celrep.2014.07.035

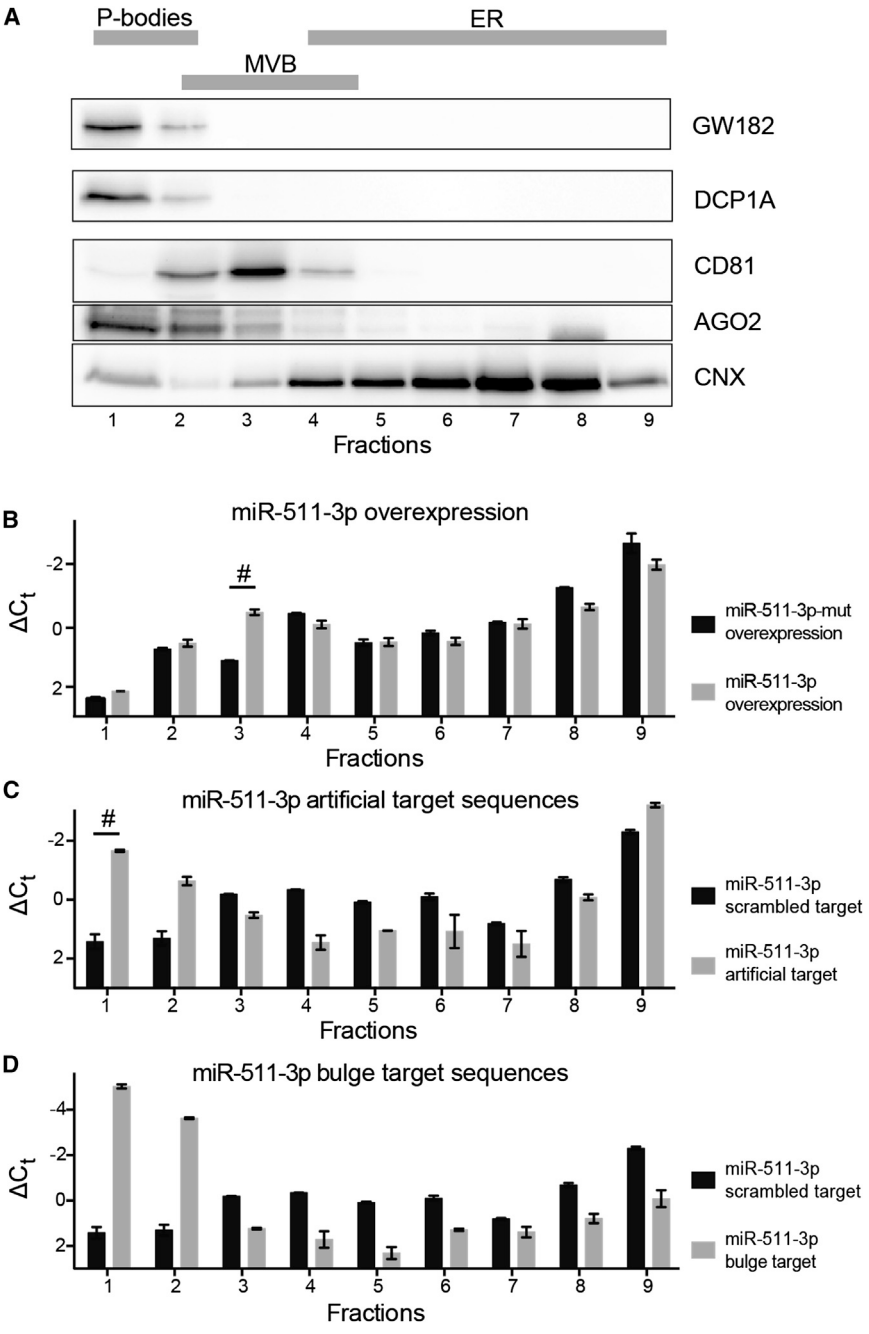

Figure 3. Relocation of miRNAs to Distinct Subcellular Compartments

(A) Western blotting analysis of subcellular fractions obtained from iBMMs. Three of six independent experiments are shown.

(B–D) miR-511-3p levels in subcellular fractions obtained from iBMMs transduced with LVs overexpressing miR-511-3p (B, versus miR-511-3p-mut), its artificial (perfectly complementary) target sequences (C, versus scrambled target), or its bulge (nonperfectly complementary) target sequences (D, versus scrambled target). For each fraction, miRNA levels are shown as ΔC_t values (difference between the C_t in the fraction of interest and the mean C_t calculated on all fractions). One representative experiment of three performed is shown for (B) and (C); statistical analysis of the data was performed on the three biological replicates (B and C) by two-way ANOVA, with Sidak's multiple comparison test (#$p < 0.01$).

enrichment in MVBs (miRNA secretory pathway) and P bodies (miRNA activity pathway), respectively. Thus, fluctuations of natural target levels may have the potential to relocate miRNAs from one cellular compartment to another and tilt the balance between endogenous miRNA activity and secretion through the MVB/exosome pathway.

Cell Activation Modulates miRNA:Target Interactions and Controls miRNA Sorting to Exosomes

Based on the aforementioned findings, we hypothesized that the transcriptional changes that occur in response to cell activation may control miRNA sorting to exosomes by either increasing or decreasing the pool of intracellular miRNA target sequences. To test this hypothesis, we performed RNA-seq of UT (n = 4) and IL-4-treated (n = 4) primary BMDMs. We unequivocally identified ~36,000 transcripts (including protein-coding and noncoding RNAs), of which ~21% were differentially expressed (by edgeR; adjusted p value < 0.05) in the BMDMs upon IL-4 treatment (Figure 4A; Table S3). As expected, IL-4 increased the expression of genes known to be upregulated in alternatively activated macrophages (Martinez et al., 2009), such as *Arg1*, *Retnla*, *Chi3l3* (*Ym1*), *Ccl22*, and *Mrc1* (Figure S4A).

We then implemented a computational model to investigate whether IL-4-induced changes in exo-miRNA levels (see Figures 1 and S1) were dependent on quantitative changes in miRNA target levels in the BMDMs. We first selected miRNAs with at least two out of three determinations in the qPCR array data sets of both BMDMs and exo-macs (178 miRNAs; see Figure 1). We then used the UCSC Genome Browser database (http://genome.ucsc.edu) to select transcripts that contain a 3′ UTR sequence. We identified miRNA target sites (seed:RNA interactions) in each transcript's 3′ UTR and rationally assigned a weight to each of the three main typologies of the seed:RNA interaction (8-mer > 7-mer > 6-mer) to obtain a "weighted interaction score" for each transcript (WIS_t; Supplemental Experimental Procedures). Although 5′ UTRs and open reading frames (ORFs) of mammalian genes contain predicted miRNA target sites, their contribution to miRNA-mediated gene repression is deemed marginal (Bartel, 2009; Grimson et al.,

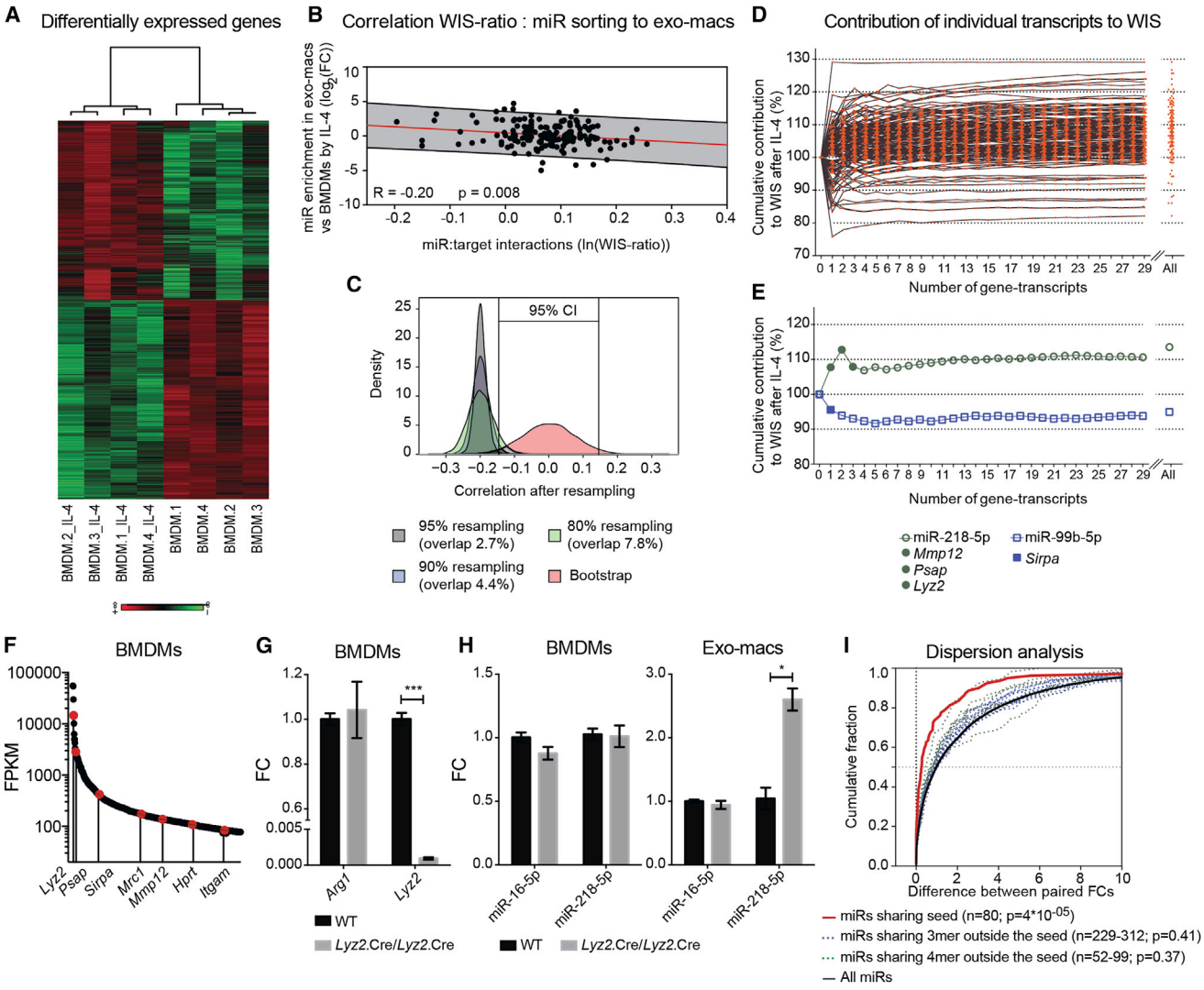

Figure 4. Gene Transcript Levels Modulate miRNA Sorting to Exo-macs

(A) Mean-centered, hierarchical clustering of genes differentially expressed in UT (BMDM.1-4) and IL-4-treated (BMDM.1-4_IL-4) BMDMs.

(B) Correlation between the WIS-ratio [shown as ln(WIS-ratio)] and miRNA (indicated as miR) enrichment in exo-macs [versus BMDMs; shown as $\log_2$(FC) of miRNA levels] after IL-4 treatment of BMDMs. The gray area identifies 95% of the events (95% prediction band).

(C) Bootstrap analysis of the data in (B) performed by randomly assigning $\log_2$(FC) to ln(WIS-ratio) values for 10^4 times (red curve, showing the distribution of R values). The black, blue, and green curves show the distribution of R values obtained by removing 20%, 10%, and 5%, respectively, of the ln(WIS-ratio) and $\log_2$(FC) values from the analysis in (B). The overlap between the random distribution and the resample distribution is indicated. The vertical lines identify confidence interval (CI = 95%).

(D and E) Cumulative contribution of individual transcripts to the WIS (D, all detected miRNAs; E, selected miRNAs) in IL-4-treated versus UT BMDMs.

(F) Transcripts with FPKM values >80 as detected in BMDMs by RNA-seq. Selected transcripts are indicated.

(G) TaqMan analysis of the indicated genes (normalized to *B2m*) in IL-4–treated BMDMs. Data show mean values (±SEM, n = 3). Statistical analysis by unpaired Student's t test.

(H) TaqMan analysis of miR-16-5p and miR-218-5p (normalized to U6) in IL-4-treated BMDMs (left) and their exo-macs (right). Data show mean values (±SEM, n = 3). Statistical analysis by unpaired Student's t test.

(I) Cumulative distribution of the difference between FC values (Δ-FC; see Figure 1F and Table S2E) of individual miRNA pairs sharing the same seed sequence (nucleotides in position 2–8; red line), all 3-mer/4-mer sequences outside the seed (blue/green lines), or randomly selected miRNA pairs (black line). Statistical analysis by Kolmogorov-Smirnov test.

2007); therefore, only 3′ UTR sequences were analyzed. We then used fragments per kilobase per million of reads (FPKM) data to determine, for each miRNA, the weighted interaction score at the transcriptome-wide level (referred to as WIS) in either UT or IL-4-treated BMDMs. Lastly, we calculated the ratio between WIS values in IL-4-treated and UT BMDMs (WIS-ratio). Based on this model, miRNAs whose predicted targets are decreased in BMDMs by IL-4 have a WIS-ratio < 1, or ln(WIS-ratio) < 0,

Please cite this article in press as: Squadrito et al., Endogenous RNAs Modulate MicroRNA Sorting to Exosomes and Transfer to Acceptor Cells, Cell Reports (2014), http://dx.doi.org/10.1016/j.celrep.2014.07.035

whereas miRNAs whose predicted targets are increased in BMDMs by IL-4 have a WIS-ratio > 1, or ln(WIS-ratio) > 0.

Interestingly, we found a weak but statistically significant anti-correlation ($p < 0.008$) between the WIS-ratio values of miRNAs and their enrichment in the exo-macs (Figures 4B and 4C). The observed anticorrelation was verified also when we employed Δ-WIS values ($p < 0.01$), which measure the absolute increase or decrease (Δ) of the WIS of each miRNA in the transcriptome of IL-4-treated versus UT BMDMs (Figure S4B). Thus, miRNAs whose predicted targets are globally decreased in BMDMs by IL-4 appear to be preferentially enriched in exosomes, and vice versa. It should be noted that we did not observe a statistically significant correlation between WIS-ratio values and differential miRNA expression in IL-4-treated versus UT BMDMs (Figure S4C), suggesting that cell-activation-dependent changes of miRNA target abundance do not globally impact on the cellular miRNA levels.

We then studied the contribution of individual transcripts to the WIS of each of the 178 selected miRNAs. We first ranked the cellular transcripts based on the magnitude of their contribution to the WIS in IL-4-treated versus UT BMDMs (i.e., by using $\Delta\text{-WIS}_t$ values). We then monitored in silico, for each miRNA the behavior of the WIS in response to the contribution of individual transcripts. We found that, on average, the transcript with highest $\Delta\text{-WIS}_t$ could contribute to increase or decrease the WIS by ~5% (0.6%–32%; Figure 4D). For example, the matrix metalloproteinase-12 (*Mmp12*) transcript, which is targeted by miR-218-5p and upregulated ~26-fold in IL-4-treated BMDMs (Table S3), increased the WIS of miR-218-5p by ~8% (Figure 4E). Prosaposin (*Psap*; upregulated ~2-fold by IL-4; Table S3) further increased the WIS of miR-218 by ~6%, whereas lysozyme-2 (*Lyz2*; downregulated ~2-fold by IL-4; Table S3; Figure S4D) decreased it by ~4.5%. Of note, the *Mmp12*, *Psap*, and *Lyz2* transcripts are all highly expressed in BMDMs (Figure 4F). When all cellular transcripts were computed, IL-4 increased the WIS of miR-218-5p by ~13.6%. Consistent with the in silico prediction, miR-218-5p levels were relatively lower in the exo-macs derived from IL-4-treated BMDMs than UT BMDMs (see Figure 1E and Table S2E). Among the miRNAs whose WIS decreased after IL-4 was miR-99b-5p (Figure 4E), a miRNA upregulated in the exo-macs in an IL-4-dependent fashion (see Figure 1F). Of note, IL-4 stimulation of BMDMs more frequently increased than decreased the WIS of the investigated miRNAs (Figure 4D).

To validate the aforementioned in silico data, we analyzed the effects of biological *Lyz2* gene knockout on miR-218-5p sorting to exo-macs. To this aim, we used BMDMs obtained from homozygous *Lyz2*.Cre mice (Clausen et al., 1999), which lack both functional copies of *Lyz2* (Figure 4G). As predicted by our model, miR-218-5p, but not miR-16-5p, which does not have binding sites in the 3′ UTR of the *Lyz2* transcript, was enriched in the exo-macs of *Lyz2*.Cre BMDMs compared to wild-type BMDMs (Figures 4H and S4D). Of note, miR-218-5p levels were similar in wild-type and *Lyz2* null BMDMs, suggesting that the *Lyz2* transcript, while containing ~13% of all miR-218-5p binding sites in the coding and noncoding transcriptome, would not modulate the cellular levels of miR-218-5p through a sponge effect.

miRNAs belonging to the same family share the same seed sequence, which controls target recognition (Lai, 2002). Based on our model, miRNA family members should display a similar sorting pattern. To study the behavior of miRNAs that either share or not the same seed sequence, we performed an in silico analysis. We calculated the difference between pairs of fold-change values (Δ-FC) measuring miRNA increase/decrease in exo-macs versus BMDMs by IL-4 (see Figure 1F and Table S2E) for all possible miRNA pairs. We found that miRNA pairs sharing the same seed sequence displayed significantly smaller Δ-FC values than randomly selected miRNA pairs (Figure 4I). Of note, miRNA pairs sharing 3-mer or 4-mer sequences located outside the seed sequence behaved similarly to random miRNA pairs.

Taken together, our results suggest that the cellular levels of natural miRNA targets, which dynamically change in response to cell activation, may modulate miRNA enrichment in exosomes without detectably affecting the cellular miRNA levels.

Macrophage-Derived Exosomes Transfer miRNA Activity to Acceptor Endothelial Cells

Macrophages modulate EC biology and stimulate angiogenesis by secreting growth factors and matrix-remodeling enzymes (Baer et al., 2013). Furthermore, miRNA transfer via exosomes may mediate macrophage-to-EC communication and, therefore, potentially influence macrophage-regulated angiogenesis. In order to visualize and measure exo-mac transfer to ECs, we generated fluorescently labeled exo-macs by transducing iBMMs with an LV expressing a CD9 cDNA fused with either mCherry (SFFV.CD9.mCherry) or enhanced GFP (SFFV.CD9.eGFP) (Figure S5A). Fluorescence spectroscopy showed readily measurable, proteinase-resistant mCherry fluorescence in the exo-macs (Figures S5B–S5D). In order to study exo-mac transfer, we established immortalized, endothelial-like cells (iELCs) from the heart of $Dicer^{fl/fl}$ mice and treated them with increasing doses of $mCherry^+$ exo-macs. Flow cytometry of iELCs showed dose-dependent mCherry fluorescence (Figure S5E). iELCs rapidly internalized exo-macs (Figure S5F), which became evident in the cell cytoplasm as punctate mCherry staining (Figure S5G). A similar intracellular pattern of mCherry was observed when iELCs were cocultured with $CD9.mCherry^+$ iBMMs (Figure S5H). LAMP1 staining of iELCs, or their transduction with a LAMP1-eGFP fusion protein (Lysotracker), indicated that a significant proportion of the mCherry signal colocalized with late endosomes/lysosomes (Figures S5I and S5J), as previously shown in other studies (Morelli et al., 2004). Whereas these data show a rapid and dose-dependent exo-mac uptake by ECs, they also indicate that a sizable proportion of the uptaken exo-macs enter the endocytic pathway and are possibly degraded in lysosomes.

To measure exo-miRNA transfer from macrophages to ECs, we cocultured an EC line, bEND.3, with iBMMs in transwell assays. We then used low-density qPCR arrays to interrogate the miRNA transcriptomes of ECs that were cultured either alone or with iBMMs. Whereas the global miRNA transcriptome of ECs was not significantly modulated by their coculture with iBMMs (data not shown), selected miRNAs were significantly increased (Figure 5A). Of these, a sizable proportion was miRNAs that displayed a relatively high enrichment in the exo-macs compared to ECs. Indeed, miRNAs that were >10-fold

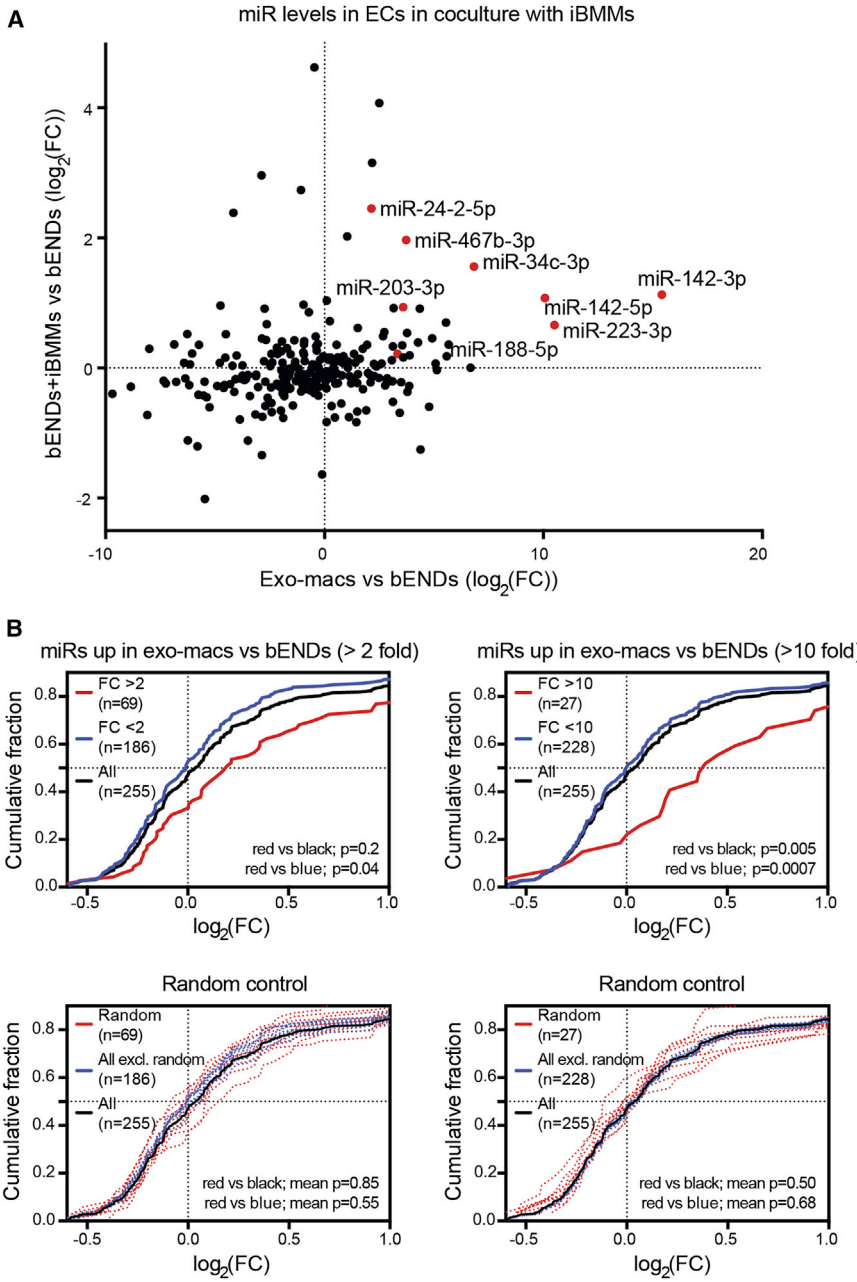

Figure 5. Global miRNA Transfer from iBMMs to ECs upon Coculture

(A) Correlation between miRNA (indicated as miR) levels in exo-macs from IL-4-treated iBMMs [$\log_2$(FC) versus bENDs; x axis] and miRNA levels in bENDs in coculture with IL-4–treated iBMMs [$\log_2$(FC) versus bENDs; y axis]. Data show independent experiments combined (n = 3 for exo-macs; n = 2 for bENDs). miRNAs of interest are indicated by red dots.

(B) Cumulative distribution of the FCs of miRNA levels in bENDs in coculture with IL-4-treated iBMMs versus bENDs. The black lines show FCs of all miRs; the red lines show FCs of miRNAs that are upregulated in exo-macs from IL-4-treated iBMMs versus bENDs by >2-fold (top left) or >10-fold (top right); the blue lines show FCs of miRNAs that are upregulated in exo-macs from IL-4-treated iBMMs versus bENDs by <2-fold (top left) or <10-fold (top right). Bottom panels show cumulative FCs using randomly selected miRNAs (using the same number of miRNAs analyzed in the top panels). Statistical analysis by two-sided Kolmogorov-Smirnov test.

higher in exo-macs than ECs were globally and significantly increased in the ECs upon coculture with iBMMs (Figure 5B). For example, miR-142-3p and miR-223-3p, which are highly expressed in iBMMs and their exo-macs but virtually undetectable in ECs, were significantly increased in ECs cocultured with iBMMs (Figure 5A). Together, these data suggest the occurrence of miRNA transfer from macrophages to ECs in vitro.

We then asked whether exo-miRNAs can repress target genes in ECs. To this aim, we constructed a panel of 32 miRNA reporter LVs, each incorporating two miRNA target (miRT) sequences with perfect complementarity to a given miRNA into the 3′ UTR of a destabilized GFP (dGFP) transgene, which is expressed from a ubiquitously active bidirectional promoter that also controls the expression of the reporter gene, ΔLNGFR (Figure S6A). We also generated a control LV expressing a dGFP sequence not containing miRT sequences in its 3′ UTR (termed no-miRT). Following LV cell transduction, the miRNA machinery will degrade the dGFP transcript containing miRT sequences only in the cells that express the cognate miRNA, in a manner that is dependent on miRNA abundance and/or activity. On the other hand, expression of ΔLNGFR is independent of miRNA activity and is used as an internal normalizer to calculate GFP fold repression as a direct readout of miRNA activity, as described previously (Brown et al., 2007; Mullokandov et al., 2012; Squadrito et al., 2012).

We first measured endogenous miRNA activity in IL-4-treated iBMMs and ECs (bEND.3). We found that several miRNAs were highly active in both cell types, such as miR-21a-5p, miR-24-3p, Let-7e-5p, and Let-7a-5p (Figure S6B). Other miRNAs showed specific and/or high activity in either cell type, such as miR-142-3p, miR-511-3p (specifically active in iBMMs), miR-92a-3p, and miR-125a-5p (highly and specifically active in ECs). In order to measure functional exo-miRNA transfer, iELCs expressing miRNA reporter LVs were incubated with exo-macs from IL-4-treated iBMMs. The exo-macs were readily uptaken by and transferred miRNA activity to iELCs (+10%–20% miRNA activity compared to cells not exposed to exo-macs; Figures S6C–S6E). To rule out de novo endogenous miRNA activity, we transduced

Please cite this article in press as: Squadrito et al., Endogenous RNAs Modulate MicroRNA Sorting to Exosomes and Transfer to Acceptor Cells, Cell Reports (2014), http://dx.doi.org/10.1016/j.celrep.2014.07.035

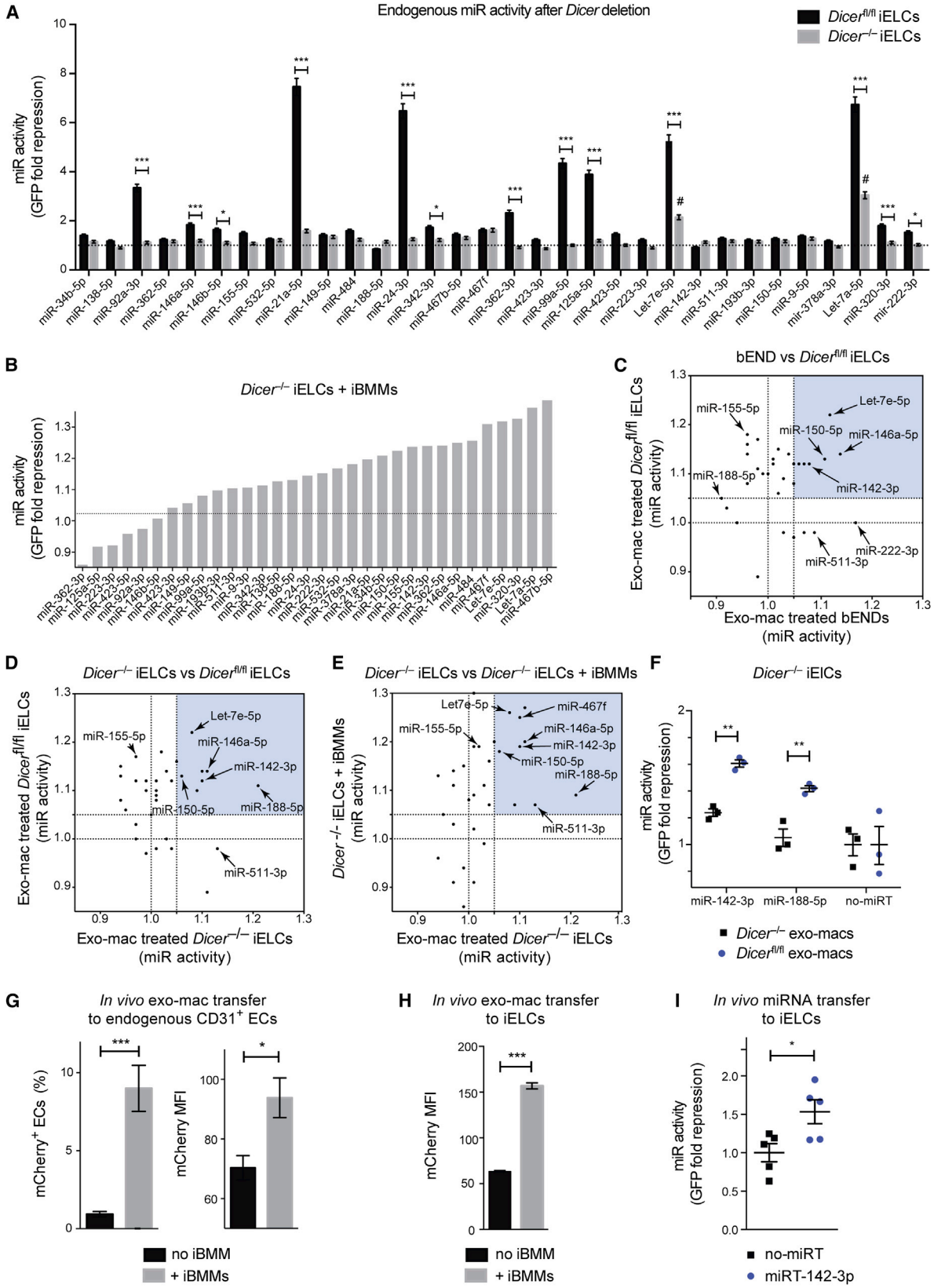

(legend on next page)

Dicer$^{fl/fl}$ iELCs with a hPGK.Cre-Puro LV (Figure S2A) and selected a *Dicer*$^{-/-}$ iELC clone for subsequent experiments (Figure S6F). As expected, endogenous miRNA activity was globally disrupted in *Dicer*$^{-/-}$ iELCs (Figure 6A), although Let-7 family members displayed residual activity, possibly due to DICER-independent miRNA processing (Cifuentes et al., 2010). Of note, we found substantially lower miRNA activity in *Dicer*$^{-/-}$ than *Dicer*$^{fl/fl}$ iELCs following their incubation with exo-macs (Figure S6G). This observation suggests that low-level exo-miRNA activity may be masked by endogenous miRNA activity induced by cell treatment with exosomes.

We then asked whether continuous exposure of ECs to macrophages would increase transfer of exo-miRNA activity. Coculturing iBMMs with *Dicer*$^{-/-}$ iELCs led to substantial transfer of miRNA activity from the macrophages to ECs (+10%–40% miRNA activity compared to cells not cocultured with iBMMs; Figure 6B). We then compared miRNA activity in different ECs (bEND.3, *Dicer*$^{fl/fl}$ and *Dicer*$^{-/-}$ iELCs) either treated with exo-macs or cocultured with iBMMs. We consistently found increased activity of selected miRNAs, including Let-7e-5p, miR-142-3p, miR-188-5p, miR-146a-5p, and miR-150-5p, in the ECs (Figures 6B–6E; Figures S6E and S6G). Of note, the aforementioned miRNAs are either highly expressed in macrophages (e.g., miR-142-3p and miR-146a-5p) or enriched in the exo-macs (e.g., miR-146a-5p, miR-188-5p, miR-150-5p, and miR-467f; see Figure 1).

We then selected two exo-miRNAs, miR-188-5p and miR-142-3p, for further validation experiments. Importantly, transfer of miRNA activity to *Dicer*$^{-/-}$ iELCs was greatly decreased when exo-macs were isolated from miRNA-depleted, *Dicer*$^{-/-}$ iBMMs (Figure 6F), demonstrating genuine transfer of exo-miRNA activity from macrophages to ECs in vitro. Finally, in order to study functional exo-miRNA transfer in vivo, we inoculated Matrigel plugs containing *Dicer*$^{-/-}$ iELCs transduced with a miR-142-3p reporter LV (or a no-miRT LV), with or without CD9.mCherry^{+} iBMMs, subcutaneously in athymic (*nu/nu*$^{-/-}$) mice. Eight days later, we analyzed the Matrigel plugs by flow cytometry. Both the percentage and mCherry mean fluorescence intensity (MFI) of the endogenous CD31^{+} ECs were significantly higher in implants containing CD9.mCherry^{+} iBMMs (Figure 6G), therefore showing exo-mac fusion with ECs in vivo. Moreover, both the mCherry MFI and miR-142-3p activity were increased in the *Dicer*$^{-/-}$ iELCs from implants containing CD9.mCherry^{+} iBMMs (Figures 6H and 6I), indicating bona fide transfer of exo-miRNA activity from macrophages to ECs in vivo.

DISCUSSION

The results of this study suggest that miRNA availability for exosomal secretion is controlled, at least in part, by the cellular levels of their targeted transcripts. By employing both transcriptomic analyses and LV-reporter based assays, we found that either physiological (cell-activation-dependent) or artificial overexpression of miRNA target sequences promotes a relative miRNA enrichment in P-bodies and depletion from MVBs and exosomes. Conversely, artificial overexpression of a miRNA enriches it in MVBs and exosomes. These results were corroborated by implementing a computational model to identify miRNA:target interactions at the genome-wide level. IL-4-stimulated macrophages were selected as a cellular system based on our finding, as well as extensive previous work (Martinez et al., 2009), that IL-4 activates macrophages by skewing the expression of a large proportion of genes. By comparing IL-4-treated and UT macrophages, the model revealed a statistically significant, negative correlation between miRNA:target interactions in the cells and miRNA enrichment in exosomes. These findings may imply that exosomal miRNA secretion is a mechanism whereby cells rapidly dispose miRNAs in excess of their targets to adjust miRNA:mRNA homeostasis.

miRNA:mRNA interactions were computed by considering canonical seed:target matches predicted to occur among all miRNAs and gene transcripts that were detected in our transcriptomic data sets. Although short-sequence interactions (6-mers) account for the vast majority of the predicted seed:target matches (~70%), they contain many false positives and have low specificity and precision (Ellwanger et al., 2011). miRNA:target prediction algorithms like TargetScan therefore favor seed:target matches with longer over shorter sequence (Ellwanger et al., 2011; Grimson et al., 2007). To take these considerations into account, the three main categories of seed:target matches (i.e., 6-mer, 7-mer, and 8-mer) were assigned a weighted score (0.3, 0.7, and 1.0, respectively) to minimize the contribution of false positives (which are more prevalent among 6-mers) and emphasize that of the most robust seed:target matches (8-mers). For the sake of simplicity, our model did not consider other miRNA/target features that may predict miRNA activity, such as the conservation of the seed:target match, the nucleotide composition of the seed:target flanking regions, and free energy-based determinants, among others (Wen et al., 2011). Moreover, we only considered seed:target matches in the 3′ UTR and excluded those in the 5′ UTR and

Figure 6. In Vivo Transfer of Exosomes and miRNA Activity from Macrophages to ECs

(A) Endogenous miRNA (indicated as miR) activity in *Dicer*$^{fl/fl}$ (n = 2) and *Dicer*$^{-/-}$ iELCs (n = 4) measured by miRNA reporter LVs, shown as GFP fold-repression normalized to iELCs transduced with a no-miRT control LV. Statistical analysis by two-way ANOVA, with Sidak's multiple comparison test. # indicates miRNAs that display activity after *Dicer* deletion.

(B) miRNA activity in *Dicer*$^{-/-}$ iELCs in coculture with iBMMs (versus *Dicer*$^{-/-}$ iELCs; n = 2), measured by miRNA reporter LVs (normalized to a no-miRT LV).

(C–E) miRNA activity in either iELCs or bENDs treated as indicated (versus UT), measured by miRNA reporter LVs (normalized to a no-miRT LV). miRNAs in the blue quadrant are recurrently increased in the ECs both by exo-mac treatment and coculture with iBMMs.

(F) miR-142-3p and miR-188-5p activity (normalized to a no-miRT LV) in *Dicer*$^{-/-}$ iELCs treated with exo-macs from either *Dicer*$^{fl/fl}$ or *Dicer*$^{-/-}$ iBMMs (three biological replicates and two independent experiments, of which one is shown). Statistical analysis by two-way ANOVA, with Sidak's multiple comparison test.

(G–I) Flow cytometry analysis of ECs from Matrigel plugs either containing CD9.mCherry^{+} iBMMs (n = 7) or not (n = 13). (G) Percentage of mCherry^{+} ECs (left) and mCherry MFI of endogenous CD31^{+} ECs (right); percentage values were converted to arcsin values and statistical analysis performed by unpaired t test. (H) mCherry MFI of ΔLNGFR^{+} *Dicer*$^{-/-}$ iELCs; statistical analysis by unpaired Student's t test. (I) miR-142-3p activity (normalized to a no-miRT LV) in ΔLNGFR^{+} *Dicer*$^{-/-}$ iELCs in implants containing CD9.mCherry^{+} iBMMs (n = 5); statistical analysis by unpaired Student's t test.

Please cite this article in press as: Squadrito et al., Endogenous RNAs Modulate MicroRNA Sorting to Exosomes and Transfer to Acceptor Cells, Cell Reports (2014), http://dx.doi.org/10.1016/j.celrep.2014.07.035

ORF of the transcript. Several studies have indeed shown that miRNA-binding sites in ORFs and 5′ UTRs contribute minimally to miRNA activity (Baek et al., 2008; Grimson et al., 2007); therefore, computing such interactions in our model would have likely increased the proportion of false positives. For the same reason, we did not consider noncanonical miRNA binding sites, such as bulge seed:target interactions and those containing G:U matches (Helwak et al., 2013). Because we implemented simplified criteria aimed to minimize potential false positives, it is possible that our results neglect the contribution of a fraction of the miRNA:target interactions to exo-miRNA biogenesis and hence underestimate the breadth of the phenomenon. In addition to the contribution of the aforementioned factors, the relative weakness of the anticorrelation suggests the very likely scenario that additional mechanisms regulate miRNA sorting to exosomes, such as miRNA family and sequence-specific or biogenesis-dependent mechanisms (Kosaka et al., 2010; Villarroya-Beltri et al., 2013).

Several reports have shown that miRNA activity is higher in cytoplasmic granules known as GW or P bodies, where proteins that have a key role in translation repression, such as GW182 and AGO2, have been shown to colocalize with untranslated mRNAs (Jakymiw et al., 2005; Liu et al., 2005; Pillai, 2005). Of note, GW/P bodies localize in close proximity to MVBs (Gibbings et al., 2009), which are involved in exosome biogenesis. It is therefore tempting to speculate that miRNAs may passively traffic from GW/P bodies to MVBs in response to oscillations of target mRNA levels associated with such organelles. Recent studies have also shown that miRNA activity may colocalize, at least in part, with other subcellular compartments, such as the rough ER (Stalder et al., 2013).

It has been proposed that the natural targets of a given miRNA may act as "competing endogenous RNAs" (ceRNAs) that regulate miRNA bioavailability by competing with each other for miRNA binding (Cesana et al., 2011; Poliseno et al., 2010; Tay et al., 2011, 2014). For example, it was found that the *PTEN* pseudogene, *PTENP1*, whose 3′ UTR is highly homologous to that of *PTEN* and contains many miRNA target sites, upregulates PTEN expression by competing with *PTEN* for the binding to miRNAs (Poliseno et al., 2010). In another study, a human circular RNA antisense to *CDR1* (termed *CDR1as*) operated as a miRNA antagonist by sequestering miR-7 through 63 conserved sites present in its sequence (Memczak et al., 2013). Our data (Figures 2E and 2F) are in line with previous reports that exceedingly high copies of a miRNA target are required in a cell to disrupt miRNA activity through a "sponge effect" (Baccarini et al., 2011; Brown and Naldini, 2009; Denzler et al., 2014; Gentner et al., 2009). For example, we found that the genetic knockout of *Lyz2*, which contributes to almost 3% of all the total transcripts and at least 13% of the target sites for miR-218-5p in BMDMs, did not affect the cellular levels of miR-218-5p but significantly increased its loading into exosomes. Thus, changes in endogenous target levels that are insufficient to detectably alter miRNA abundance (and possibly activity) in the cell may have the potential to modulate miRNA sorting to exosomes through a "miRNA relocation effect" likely regulated by the relative amounts of bound versus unbound miRNA and unknown mechanisms of subcellular miRNA compartmentalization (Ameres et al., 2010; Baccarini et al., 2011; Mullokandov et al., 2012).

While our findings suggest that miRNA sorting to exosomes may be a passive mechanism to dispose miRNAs in excess of their cellular targets, increasing data indicate that exosomes can be actively internalized by other cells, resulting in miRNA transfer among cells of both homo- and heterotypic nature (Hergenreider et al., 2012; Mittelbrunn et al., 2011; Ramachandran and Palanisamy, 2012; Simons and Raposo, 2009; Skog et al., 2008; Valadi et al., 2007). Furthermore, extracellular miRNAs may represent biomarkers of disease and response to therapy. For example, cancer cells display altered transcriptomic profiles, which in turn may differentially modulate miRNA sorting to exosomes. Certain miRNA signatures identified in serum exosomes indeed have both diagnostic and prognostic power for some cancer types (Manterola et al., 2014; Pigati et al., 2010; Skog et al., 2008).

Although miRNAs can traffic among cells via exosomes and other microvesicles, the significance of exogenously derived miRNAs for the global miRNA activity of a cell remains unclear. To rigorously quantitate the effects of exosome-mediated miRNA transfer in a model of macrophage-to-EC communication, we generated *Dicer*-deficient ECs and exposed them to exosomes from either *Dicer*-proficient or *Dicer*-deficient macrophages. Although we detected bona fide transfer of miRNA activity via exosomes, the contribution of exogenously derived miRNAs to target gene repression was overall modest. While our findings indicate that most of the exo-macs uptaken by ECs end up in lysosomes, suggesting degradation of their miRNA content, they do not exclude the possibility that certain tissue microenvironments, such as tumors (Baer et al., 2013) or atherosclerotic plaques (Hergenreider et al., 2012), may facilitate miRNA transfer among cells by producing profuse amounts of miRNA-enriched exosomes. Indeed, macrophages abundantly enwrap immature blood vessels in tumors, a process that may enhance exo-mac fusion with ECs and, consequently, miRNA transfer to ECs engaged in angiogenesis (Baer et al., 2013; Squadrito et al., 2013).

In summary, our data indicate that dynamic transcriptomic changes that occur in response to cell activation may modulate miRNA sorting to exosomes, at least in part, by differentially engaging them at sites of miRNA activity (P bodies) and exosome biogenesis (MVBs). Such mechanism of miRNA compartmentalization regulated by miRNA targets may have implications for exosome-mediated miRNA transfer and intercellular communication.

EXPERIMENTAL PROCEDURES

Additional or more detailed experimental procedures are available in the Supplemental Experimental Procedures.

Lentiviral Vector Construction

Detailed information (sequences, primers, and cloning strategies) is available in the Supplemental Experimental Procedures.

miRNA Reporter LVs

Thirty-two different miRNA reporter LVs were generated by introducing two tandem sequences with perfect complementarity to specific miRNAs (miRT sequences) downstream to a destabilized GFP (dGFP) transgene expressed

from a bidirectional LV also encoding for a ΔLNGFR transgene (Amendola et al., 2005).

LVs for Overexpression of miR-511-3p or Its Target Sequences

LVs to overexpress miR-511-3p, or its mutated form, were described previously (Squadrito et al., 2012). LVs to overexpress artificial or natural target sequences for miR-511-3p are based on a SFFV.dGFP LV, which exploits the strong SFFV promoter to overexpress a dGFP transgene linked to eight tandem sequences with complementarity to a given miRNA (Gentner et al., 2009). Natural target sequences for miR-511-3p were obtained from the *Rock2* 3′ UTR, as described previously (Squadrito et al., 2012).

LV to Express Cre Recombinase or Immortalize BMDMs

The Cre LV was generated by replacing the ΔLNGFR and the GFP DNA sequences of a bidirectional LV (Amendola et al., 2005) with Cre and puromycin resistance (Puro) coding sequences, respectively. The SV40 large T antigen (TAg) coding sequence (a gift from Didier Trono, EPFL) was cloned in an SFFV promoter-containing LV (Squadrito et al., 2012).

Exosome Isolation

In order to isolate exo-macs, BMDMs and iBMMs were cultured in serum-free medium (SFM medium; Life Technologies). In coculture experiments (e.g., iBMMs with ECs), culture medium was supplemented with FBS previously depleted of exosomes by ultracentrifugation at 134,000 × *g* for 6 hr. In order to isolate exo-macs, we employed two different techniques: (1) ExoQuick TC (System Biosciences), for primary BMDMs; and (2) ultracentrifugation, for iBMMs. Exo-macs were used immediately or stored at −80°C. Detailed protocols are available in Supplemental Experimental Procedures.

Low-Density miRNA TaqMan Arrays

The Rodent MicroRNA TaqMan Array (Life Technologies) was used to profile miRNAs in BMDMs; IL-4-treated BMDMs; bEND.3; bEND.3 cocultured with macrophages; exo-macs from UT BMDMs; and exo-macs from IL-4-treated BMDMs. The data were collected and processed using the SDS2.4 software (Life Technologies). miRNAs that had fewer than two out of three determinations per condition were excluded from the analysis. C_t values were normalized using the quantile method. Additional information is available in the Supplemental Experimental Procedures.

RNA-Seq of BMDMs

UT (n = 4) and IL-4-treated (n = 4) BMDMs were lysed in Qiazol and total RNA extracted. Total RNA was then depleted of rRNA using the Ribo-Zero RNA removal kit (Epicenter Biotechnologies). Illumina sequencing libraries were prepared according to the TruSeq RNA v2 Sample Preparation Guide (Revision B) and sequencing performed on a HiSeq 2500 (Illumina) using paired-end cBot v3 clustering and TruSeq SBS reagents. Libraries were sequenced using 2 × 100 bp paired-end reads. The 100 nt paired-end reads were then mapped to mm9 reference genome using Tophat software version 2.0.9, with default options, using mm9 UCSC reference genes GTF. Count data for each exon were generated using htseq-count from the HTseq package (http://www-huber.embl.de/users/anders/HTSeq/; version 0.5.4p3). Fragments per kilobase per million of reads (FPKM) were estimated for transcripts in each of the conditions using the cufflinks software (version 2.1.1). Additional information is available in the Supplemental Experimental Procedures.

Gene/miRNA Expression Analysis by TaqMan Arrays and RNA-Seq

Differentially expressed mature miRNAs (TaqMan arrays) and gene transcripts (RNA-seq) were identified using the limma package in R. For gene transcripts, the raw read counts per gene were first filtered for minimal expression (average of raw counts was more than five across samples), normalized to the relative size of each library using the R package edgeR, and then transformed to log2-cpm (counts per million reads) using the voom function. Empirical Bayes moderated t statistics and corresponding p values were then computed for the comparison (IL-4-treated versus UT BMDMs/exo-macs). p values were adjusted for multiple comparisons using the Benjamini Hochberg procedure. Gene transcripts and miRNAs with an adjusted $p \leq 0.05$ were considered to be differentially expressed. Additional information is available in Supplemental Experimental Procedures.

Statistical Analysis

Statistical analysis of the data is described in the figure legends. Error bars show mean values ± SEM, unless stated otherwise. Statistical significance of the data is indicated as follows: *p < 0.05; **p < 0.01; ***p < 0.001.

ACCESSION NUMBERS

RNA-seq data (eight BMDM samples) have been deposited to the NCBI Gene Expression Omnibus under accession number GSE58283.

SUPPLEMENTAL INFORMATION

Supplemental Information includes Supplemental Experimental Procedure, six figures, and three tables and can be found with this article online at http://dx.doi.org/10.1016/j.celrep.2014.07.035.

AUTHOR CONTRIBUTIONS

M.L.S. designed and performed research, constructed LVs, devised the bioinformatic model for analyzing miRNA:target interactions, analyzed data, and wrote the manuscript. C.B. designed and performed research, analyzed data, and wrote the manuscript. F.B. and M.I. analyzed RNA-seq and miRNA TaqMan array raw data and developed (along with M.L.S.) the bioinformatic model for analyzing miRNA:target interactions. C.M. performed research and produced LVs. G.D.G. and R.L. performed RNA-seq. M.D.P. coordinated and supervised research, analyzed the data, and wrote the manuscript with input from all authors.

ACKNOWLEDGMENTS

We thank Luigi Naldini for sharing LV constructs, Ioannis Xenarios for support with bioinformatic studies, and M. Luisa Iruela-Arispe for help with the Matrigel plug experiments. This work was funded by Fonds National Suisse de la Recherche Scientifique (SNSF grant 31003A-143978), the National Center of Competence in Research (NCCR) in Molecular Oncology, the European Research Council (ERC Staring Grant Tie2+Monocytes), and Anna Fuller Fund (to M.D.P.). F.B. and M.I. were supported in part by the Swiss Federal Government through the State Secretariat for Education, Research and Innovation (SERI).

Received: May 8, 2014
Revised: July 1, 2014
Accepted: July 22, 2014
Published: August 21, 2014

REFERENCES

Amendola, M., Venneri, M.A., Biffi, A., Vigna, E., and Naldini, L. (2005). Coordinate dual-gene transgenesis by lentiviral vectors carrying synthetic bidirectional promoters. Nat. Biotechnol. *23*, 108–116.

Ameres, S.L., Martinez, J., and Schroeder, R. (2007). Molecular basis for target RNA recognition and cleavage by human RISC. Cell *130*, 101–112.

Ameres, S.L., Horwich, M.D., Hung, J.H., Xu, J., Ghildiyal, M., Weng, Z., and Zamore, P.D. (2010). Target RNA-directed trimming and tailing of small silencing RNAs. Science *328*, 1534–1539.

Baccarini, A., Chauhan, H., Gardner, T.J., Jayaprakash, A.D., Sachidanandam, R., and Brown, B.D. (2011). Kinetic analysis reveals the fate of a microRNA following target regulation in mammalian cells. Curr. Biol. *21*, 369–376.

Baek, D., Villén, J., Shin, C., Camargo, F.D., Gygi, S.P., and Bartel, D.P. (2008). The impact of microRNAs on protein output. Nature *455*, 64–71.

Baer, C., Squadrito, M.L., Iruela-Arispe, M.L., and De Palma, M. (2013). Reciprocal interactions between endothelial cells and macrophages in angiogenic vascular niches. Exp. Cell Res. *319*, 1626–1634.

Bartel, D.P. (2009). MicroRNAs: target recognition and regulatory functions. Cell *136*, 215–233.

Please cite this article in press as: Squadrito et al., Endogenous RNAs Modulate MicroRNA Sorting to Exosomes and Transfer to Acceptor Cells, Cell Reports (2014), http://dx.doi.org/10.1016/j.celrep.2014.07.035

Brown, B.D., and Naldini, L. (2009). Exploiting and antagonizing microRNA regulation for therapeutic and experimental applications. Nat. Rev. Genet. *10*, 578–585.

Brown, B.D., Gentner, B., Cantore, A., Colleoni, S., Amendola, M., Zingale, A., Baccarini, A., Lazzari, G., Galli, C., and Naldini, L. (2007). Endogenous microRNA can be broadly exploited to regulate transgene expression according to tissue, lineage and differentiation state. Nat. Biotechnol. *25*, 1457–1467.

Cesana, M., Cacchiarelli, D., Legnini, I., Santini, T., Sthandier, O., Chinappi, M., Tramontano, A., and Bozzoni, I. (2011). A long noncoding RNA controls muscle differentiation by functioning as a competing endogenous RNA. Cell *147*, 358–369.

Cifuentes, D., Xue, H., Taylor, D.W., Patnode, H., Mishima, Y., Cheloufi, S., Ma, E., Mane, S., Hannon, G.J., Lawson, N.D., et al. (2010). A novel miRNA processing pathway independent of Dicer requires Argonaute2 catalytic activity. Science *328*, 1694–1698.

Clausen, B.E., Burkhardt, C., Reith, W., Renkawitz, R., and Förster, I. (1999). Conditional gene targeting in macrophages and granulocytes using LysMcre mice. Transgenic Res. *8*, 265–277.

Denzler, R., Agarwal, V., Stefano, J., Bartel, D.P., and Stoffel, M. (2014). Assessing the ceRNA hypothesis with quantitative measurements of miRNA and target abundance. Mol. Cell *54*, 766–776.

Ellwanger, D.C., Büttner, F.A., Mewes, H.W., and Stümpflen, V. (2011). The sufficient minimal set of miRNA seed types. Bioinformatics *27*, 1346–1350.

Gentner, B., Schira, G., Giustacchini, A., Amendola, M., Brown, B.D., Ponzoni, M., and Naldini, L. (2009). Stable knockdown of microRNA in vivo by lentiviral vectors. Nat. Methods *6*, 63–66.

Gibbings, D.J., Ciaudo, C., Erhardt, M., and Voinnet, O. (2009). Multivesicular bodies associate with components of miRNA effector complexes and modulate miRNA activity. Nat. Cell Biol. *11*, 1143–1149.

Grimson, A., Farh, K.K., Johnston, W.K., Garrett-Engele, P., Lim, L.P., and Bartel, D.P. (2007). MicroRNA targeting specificity in mammals: determinants beyond seed pairing. Mol. Cell *27*, 91–105.

Guduric-Fuchs, J., O'Connor, A., Camp, B., O'Neill, C.L., Medina, R.J., and Simpson, D.A. (2012). Selective extracellular vesicle-mediated export of an overlapping set of microRNAs from multiple cell types. BMC Genomics *13*, 357.

Helwak, A., Kudla, G., Dudnakova, T., and Tollervey, D. (2013). Mapping the human miRNA interactome by CLASH reveals frequent noncanonical binding. Cell *153*, 654–665.

Hergenreider, E., Heydt, S., Tréguer, K., Boettger, T., Horrevoets, A.J., Zeiher, A.M., Scheffer, M.P., Frangakis, A.S., Yin, X., Mayr, M., et al. (2012). Atheroprotective communication between endothelial cells and smooth muscle cells through miRNAs. Nat. Cell Biol. *14*, 249–256.

Jakymiw, A., Lian, S., Eystathioy, T., Li, S., Satoh, M., Hamel, J.C., Fritzler, M.J., and Chan, E.K. (2005). Disruption of GW bodies impairs mammalian RNA interference. Nat. Cell Biol. *7*, 1267–1274.

Kosaka, N., Iguchi, H., Yoshioka, Y., Takeshita, F., Matsuki, Y., and Ochiya, T. (2010). Secretory mechanisms and intercellular transfer of microRNAs in living cells. J. Biol. Chem. *285*, 17442–17452.

Lai, E.C. (2002). Micro RNAs are complementary to 3′ UTR sequence motifs that mediate negative post-transcriptional regulation. Nat. Genet. *30*, 363–364.

Lewis, B.P., Burge, C.B., and Bartel, D.P. (2005). Conserved seed pairing, often flanked by adenosines, indicates that thousands of human genes are microRNA targets. Cell *120*, 15–20.

Liu, J., Valencia-Sanchez, M.A., Hannon, G.J., and Parker, R. (2005). MicroRNA-dependent localization of targeted mRNAs to mammalian P-bodies. Nat. Cell Biol. *7*, 719–723.

Manterola, L., Guruceaga, E., Gállego Pérez-Larraya, J., González-Huarriz, M., Jauregui, P., Tejada, S., Diez-Valle, R., Segura, V., Samprón, N., Barrena, C., et al. (2014). A small noncoding RNA signature found in exosomes of GBM patient serum as a diagnostic tool. Neuro-oncol. *16*, 520–527.

Martinez, F.O., Helming, L., and Gordon, S. (2009). Alternative activation of macrophages: an immunologic functional perspective. Annu. Rev. Immunol. *27*, 451–483.

Memczak, S., Jens, M., Elefsinioti, A., Torti, F., Krueger, J., Rybak, A., Maier, L., Mackowiak, S.D., Gregersen, L.H., Munschauer, M., et al. (2013). Circular RNAs are a large class of animal RNAs with regulatory potency. Nature *495*, 333–338.

Mittelbrunn, M., Gutiérrez-Vázquez, C., Villarroya-Beltri, C., González, S., Sánchez-Cabo, F., González, M.A., Bernad, A., and Sánchez-Madrid, F. (2011). Unidirectional transfer of microRNA-loaded exosomes from T cells to antigen-presenting cells. Nat Commun *2*, 282.

Montecalvo, A., Larregina, A.T., Shufesky, W.J., Stolz, D.B., Sullivan, M.L., Karlsson, J.M., Baty, C.J., Gibson, G.A., Erdos, G., Wang, Z., et al. (2012). Mechanism of transfer of functional microRNAs between mouse dendritic cells via exosomes. Blood *119*, 756–766.

Morelli, A.E., Larregina, A.T., Shufesky, W.J., Sullivan, M.L., Stolz, D.B., Papworth, G.D., Zahorchak, A.F., Logar, A.J., Wang, Z., Watkins, S.C., et al. (2004). Endocytosis, intracellular sorting, and processing of exosomes by dendritic cells. Blood *104*, 3257–3266.

Mullokandov, G., Baccarini, A., Ruzo, A., Jayaprakash, A.D., Tung, N., Israelow, B., Evans, M.J., Sachidanandam, R., and Brown, B.D. (2012). High-throughput assessment of microRNA activity and function using microRNA sensor and decoy libraries. Nat. Methods *9*, 840–846.

Nolte-'t Hoen, E.N., Buermans, H.P., Waasdorp, M., Stoorvogel, W., Wauben, M.H., and 't Hoen, P.A. (2012). Deep sequencing of RNA from immune cell-derived vesicles uncovers the selective incorporation of small non-coding RNA biotypes with potential regulatory functions. Nucleic Acids Res. *40*, 9272–9285.

Pigati, L., Yaddanapudi, S.C., Iyengar, R., Kim, D.J., Hearn, S.A., Danforth, D., Hastings, M.L., and Duelli, D.M. (2010). Selective release of microRNA species from normal and malignant mammary epithelial cells. PLoS ONE *5*, e13515.

Pillai, R.S. (2005). MicroRNA function: multiple mechanisms for a tiny RNA? RNA *11*, 1753–1761.

Poliseno, L., Salmena, L., Zhang, J., Carver, B., Haveman, W.J., and Pandolfi, P.P. (2010). A coding-independent function of gene and pseudogene mRNAs regulates tumour biology. Nature *465*, 1033–1038.

Ramachandran, S., and Palanisamy, V. (2012). Horizontal transfer of RNAs: exosomes as mediators of intercellular communication. Wiley Interdiscip Rev RNA *3*, 286–293.

Simons, M., and Raposo, G. (2009). Exosomes—vesicular carriers for intercellular communication. Curr. Opin. Cell Biol. *21*, 575–581.

Skog, J., Würdinger, T., van Rijn, S., Meijer, D.H., Gainche, L., Sena-Esteves, M., Curry, W.T., Jr., Carter, B.S., Krichevsky, A.M., and Breakefield, X.O. (2008). Glioblastoma microvesicles transport RNA and proteins that promote tumour growth and provide diagnostic biomarkers. Nat. Cell Biol. *10*, 1470–1476.

Squadrito, M.L., Pucci, F., Magri, L., Moi, D., Gilfillan, G.D., Ranghetti, A., Casazza, A., Mazzone, M., Lyle, R., Naldini, L., and De Palma, M. (2012). miR-511-3p modulates genetic programs of tumor-associated macrophages. Cell Rep *1*, 141–154.

Squadrito, M.L., Etzrodt, M., De Palma, M., and Pittet, M.J. (2013). MicroRNA-mediated control of macrophages and its implications for cancer. Trends Immunol. *34*, 350–359.

Stalder, L., Heusermann, W., Sokol, L., Trojer, D., Wirz, J., Hean, J., Fritzsche, A., Aeschimann, F., Pfanzagl, V., Basselet, P., et al. (2013). The rough endoplasmatic reticulum is a central nucleation site of siRNA-mediated RNA silencing. EMBO J. *32*, 1115–1127.

Tay, Y., Kats, L., Salmena, L., Weiss, D., Tan, S.M., Ala, U., Karreth, F., Poliseno, L., Provero, P., Di Cunto, F., et al. (2011). Coding-independent regulation of the tumor suppressor PTEN by competing endogenous mRNAs. Cell *147*, 344–357.

Tay, Y., Rinn, J., and Pandolfi, P.P. (2014). The multilayered complexity of ceRNA crosstalk and competition. Nature *505*, 344–352.

Turchinovich, A., Weiz, L., and Burwinkel, B. (2012). Extracellular miRNAs: the mystery of their origin and function. Trends Biochem. Sci. *37*, 460–465.

Valadi, H., Ekström, K., Bossios, A., Sjöstrand, M., Lee, J.J., and Lötvall, J.O. (2007). Exosome-mediated transfer of mRNAs and microRNAs is a novel mechanism of genetic exchange between cells. Nat. Cell Biol. *9*, 654–659.

Villarroya-Beltri, C., Gutiérrez-Vázquez, C., Sánchez-Cabo, F., Pérez-Hernández, D., Vázquez, J., Martin-Cofreces, N., Martinez-Herrera, D.J., Pascual-Montano, A., Mittelbrunn, M., and Sánchez-Madrid, F. (2013). Sumoylated hnRNPA2B1 controls the sorting of miRNAs into exosomes through binding to specific motifs. Nat Commun *4*, 2980.

Wen, J., Parker, B.J., Jacobsen, A., and Krogh, A. (2011). MicroRNA transfection and AGO-bound CLIP-seq data sets reveal distinct determinants of miRNA action. RNA *17*, 820–834.

Yates, L.A., Norbury, C.J., and Gilbert, R.J. (2013). The long and short of microRNA. Cell *153*, 516–519.